POLARITON PEAKS FROM THE COUPLED SYSTEM OF THE SPIN TRIPLET TRANSITION AND THE CAVITY, CLASSICALY CONSIDERED IN THE LINEAR APPROXIMATION

Nathalie Fokina[1], Maia Elizbarashvili[2*]

[1]Institute "Talgha" of Georgian Technical University, Science Department, Tbilisi, Georgia

[2]Vladimir Chavchanidze Institute of Cybernetics of Georgian Technical University, Science Department, Tbilisi, Georgia

[*]Correspondence: maikoeliz@gmail.com

Abstract

Investigation of the spin-cavity polaritons (SCP) is important since they play decisive role for the creating long-storage quantum memories and optical interfaces, polaritonic chemistry and for the elaborating of masers, especially those which operate at room temperature being of the great significance for a lot of different applications. In this report, we suggest almost completely classical model for the description of the polaritonic peaks conditioned both by free and forced Rabi oscillations of the SCP system. Our investigation is based on the linearized coupled differential equations we derived semi-classically for the magnetization component of the transition of the spin triplet states and the varying field in a cavity, when the empty cavity is exactly tuned to the transition. The normal frequencies of this system of equations were found and the corresponding graphs were constructed for the appropriate values of the parameters. It is shown that the increase of the spin-photon coupling can cause both pushing apart normal frequencies at a mutual decay rate (which is the known effect), and merging together normal decay rates at a mutual frequency (which is the predicted here effect). Polariton peaks observable by the cavity transmission function and by electron paramagnetic resonance (EPR) in the form of absorption and dispersion signals were also investigated and corresponding graphs were constructed. At that, instead of a transition of spin triplet states, a variety of other two-level systems (atoms, molecules, excitons and so on) can act as emitters. Since the value of the spin-photon coupling is of great interest for applied scientists, obtaining this value by comparing our results with experimental data is of great importance.

Keywords: Polariton peaks, Rabi oscillations, Transmission function, EPR signals, Spin-photon coupling

INTRODUCTION

The photon-matter hybrid states, considered as quasiparticles, called polaritons, are typically materializing as a normal-mode splitting of the coupled radiation-matter system, where photons act on the radiation side, and emitters act on the matter side. The paradigm of *N* quantum emitters coupled to a single cavity mode and performing Rabi oscillations, appears in many situations ranging from quantum technologies to polaritonic chemistry (Haroche, 2006 and references therein), including maser generation from spin triplet states, especially those which operate at room temperature being of the great significance for a lot of different applications. Polariton peaks can be observed by the cavity transmission function and by EPR in the form of absorption and dispersion signals. From the above it follows that the purpose of the study of this paper - investigation of the polariton peaks with the help of EPR and transmission function from the coupled system of spin triplet state transition and cavity is of significant theoretical and practical interest. To achieve this goal, we almost throughout the paper use the classical approach in the linear approximation.

FORMULATION OF THE PROBLEM AND METHODS

Dynamics of the coupled system "STS transition + cavity" under the action of the steady-state weak probe microwave (MW) field is described by us with the help of the following system of differential equations for the field $B_{\mathbf{K}}^{i-j}$ and magnetization $M_{\mathbf{K}}^{i-j}$ inside the sample, basing on Ref. by Fokina and Elizbarashvili (2021)

https://doi.org/10.32388/PCGTO4.2

$$
\begin{aligned}
&d^2B_{\mathbf{K}}^{i-j}/dt^2+2\tau_c^{-1}dB_{\mathbf{K}}^{i-j}/dt+\omega_c^2B_{\mathbf{K}}^{i-j}=\eta_0\mu_0\omega_p dH_{\mathbf{K}}^{i-j}\left(probe\right)/dt-\eta_0\mu_0 d^2M_{\mathbf{K}}^{i-j}/dt^2\\
&d^2M_{\mathbf{K}}^{i-j}/dt^2+2T_2^{-1}dM_{\mathbf{K}}^{i-j}/dt+\omega_0^2M_{\mathbf{K}}^{i-j}-4\left(\eta_0\mu_0\right)^{-1}T_R^{-1}\tau_c^{-1}B_{\mathbf{K}}^{i-j}=0
\end{aligned}
\tag{1}
$$

where ω_0, ω_c are the frequencies of an spin triplet state (STS) *i-j* transition and of an empty cavity, respectively; T_2^{-1}, τ_c^{-1} are decay rates of the *i-j* transition and of a cavity, respectively; $H_{\mathbf{K}}^{i-j}\left(probe\right)$ is the probe field of the frequency ω_p in the cavity; $\left(T_R^{i-j}\right)^{-1}$ is the reciprocal radiation damping time (Abragam, 2006), written here for a cavity containing a sample possessing STSs, μ_0 is the magnetic constant; $\eta_0\le 1$ is the coefficient of the mutual overlapping of the resonance MW field mode and spin mode.

It should be mentioned that the coherent dynamics description with the help of Eqs. (1) is possible only for the case, when $\tau_c^{-1}>T_2^{-1}$(Fokina and Elizbarashvili, 2021).

$$
\left(T_R^{i-j}\right)^{-1}=\left[\mu_0 h^{-1}\left(g_K^{i-j}\mu_B\right)^2 NQP^{i-j}/V_m\right]\left\{\left(\tau_c^{-1}\right)^2/\left[\left(\tau_c^{-1}\right)^2+\left[\left(\omega_0^{i-j}\right)^2-\left(\omega_c\right)^2\right]\right]\right\},
\tag{2}
$$

where P^{i-j} and $g_{\mathbf{K}}^{i-j}$ are the polarization and the g-factor of *i-j* transition; V_m is the volume of the resonant magnetic mode; N is the full number of spins. The solution of (1) was sought in the rotating wave approximation in the form: $M_{\mathbf{K}}^{i-j}=m_{\mathbf{K}}^{i-j}e^{i\omega_p t}$; $B_{\mathbf{K}}^{i-j}=\eta_0\mu_0 h_{\mathbf{K}}^{i-j}e^{i\omega_p t}$; $H_{\mathbf{K}}^{i-j}\left(probe\right)=h_{\mathbf{K}}^{i-j}\left(probe\right)e^{i\omega_p t}$. The system of equations (1) is linear one and valid, when the slow $m_p^{i-j}=-g_{\mathbf{K}}^{i-j}\mu_B NP^{i-j}/V_m$ component of magnetization does not change under the action of the probe field ─ this means that hereafter we use the linear approximation. At that, the slow complex variables $m_{\mathbf{K}}^{i-j}$, $h_{\mathbf{K}}^{i-j}$ are the solutions of two algebraic equations, which we have written in the form for the oscillation amplitudes of two coupled oscillators (Migulin et al., 1978) under the action of a harmonic external force (further text goes without indexes *i-j*, although they are implied):

$$
\begin{aligned}
&h_{\mathbf{K}}\left(probe\right)=im_{\mathbf{K}}+i\left[\Delta_{pc}-i\theta_c\right]h_{\mathbf{K}}\\
&\left(\Delta_{p0}-i\theta_0\right)m_{\mathbf{K}}+\alpha_1\alpha_2 h_{\mathbf{K}}=0
\end{aligned}
\tag{3}
$$

$$
\Delta_{pc}=\left(1-\frac{\omega_c^2}{\omega_p^2}\right);\ \theta_c=\frac{2\tau_c^{-1}}{\omega_p}\quad \Delta_{p0}=\left(1-\frac{\omega_0^2}{\omega_p^2}\right);\ \theta_0=\frac{2T_2^{-1}}{\omega_p};\ \alpha_1\alpha_2=4T_R^{-1}\tau_c^{-1}/\omega_p^2=4g_s^2N/\omega_p^2\equiv 4\Omega_R^2/\omega_p^2.
\tag{4}
$$

$$
g_s=\sqrt{\mu_0 h^{-1}\left(g_{\mathbf{K}}\mu_B\right)^2 P^{i-j}\omega_c/2V_m}
\tag{5}
$$

is the spin-photon coupling value of a single emitter (Breeze et al, 2017).

$$
\Omega_R=\sqrt{T_R^{-1}\tau_c^{-1}}=g_s\sqrt{N},
\tag{6}
$$

where Ω_R is the Rabi frequency of a cavity with N emitters in it, having each g_s spin-photon coupling, $T_R^{-1}$is the reciprocal radiation damping time of a resonant cavity ($\omega_c=\omega_0$) with emitters in it and with the decay $\tau_c^{-1}=\omega_c/2Q$. Eq. (6) is written in two forms ─ the classical one (Fokina and Elizbarashvili, 2022) and that of cavity quantum electrodynamics (cQED) (Breeze et al., 2017) with the difference that there is an additional factor $\sqrt{P^{i-j}}$ in our formula for g_s. Eq. (6) is the main one for the transition between the both forms of the description of the coupled system "emitters + cavity".

SPECTRUM OF FREE OSCILLATIONS OF THE COUPLED SYSTEM "EMITTERS + CAVITY"

First of all, we were interested in the spectrum of the free oscillations of a coupled system "emitters + cavity", the latter being given by the equating the determinant of (3) with $\omega_p = \omega$ to zero:

$$(\Delta_1 - i\theta_1)(\Delta_2 - i\theta_2) - \alpha_1\alpha_2 = 0, \tag{7}$$

where Δ_1, Δ_2 are the complex relative detunings. Supposing $\Delta_{1,2} \to \Delta'_{1,2} + i\Delta''_{1,2}$, the following results were obtained:

1. If $\Delta'_1, \Delta'_2 \neq 0$, the frequencies of the two coupled oscillators are pushed aside by the spin-photon coupling (Figure 1):

$$\omega_\pm'^2 \equiv (2\pi)^2 \nu_\pm'^2 = \left[(\omega_0^2 + \omega_c^2) \pm \sqrt{(\omega_0^2 - \omega_c^2)^2 + 16\omega_0^2\Omega_R^2}\right]/2; \qquad \Delta''_1 = \theta_1; \quad \Delta''_2 = \theta_2, \tag{8}$$

while the corresponding rates of decay stay non-modified by it**.** It should be mentioned that $\omega_-'^2$ corresponds to the case, when emitters and the cavity field oscillate in phase, while $\omega_+'^2$ corresponds to the case of their opposite phase oscillation. Using parameters of the Ref. of Breeze et al. (2017) experiments, the following plot of the repulsion of normal frequencies was obtained by us (Figure 1).

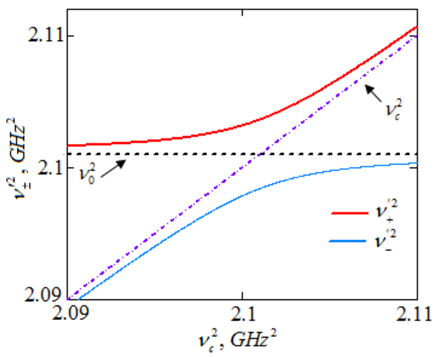

Figure 1. Repulsion of the normal frequencies $\nu_+'^2$ and $\nu_-'^2$ of the coupled system "STS Z-X transition + cavity" of 0.053% mol/mol pentacene-doped p-terphenyl crystal, plotted according to Eq. (8) of the given paper at the following values of the parameters: $\Omega_R = 2\pi \times 0.9 MHz$**;** $|\omega_0^{Z-X}| = 2\pi \times 1449.5 MHz$ (Breeze et al., 2017)

2. If $\Delta'_1 \cdot \Delta'_2 = 0$, two coupled oscillators stay with their partial frequencies, but their decays are changed. If $4\alpha_1\alpha_2 < (\theta_1 - \theta_2)^2$:

$$\omega_+ = \omega_0; \quad \omega_- = \omega_c; \quad \omega''_\pm = \frac{(T_2^{-1} + \tau_c^{-1})}{2} \pm \sqrt{\left(\frac{T_2^{-1} - \tau_c^{-1}}{2}\right)^2 - \Omega_R^2} \tag{9}$$

3. The case of level anticrossing (LAC) — the intersection point of the lines ν_0^2 and ν_c^2 in the Figure 1:

If $4\Omega_R^2 > (\tau_c^{-1} - T_2^{-1})^2$, $\quad \omega_0^2 = \omega_c^2 = \omega_{LAC}^2$, $\Delta'_{LAC} = \pm\sqrt{4\Omega_R^2 - (\tau_c^{-1} - T_2^{-1})^2}/\omega_0$, $\Delta''_{LAC} = (\tau_c^{-1} + T_2^{-1})/\omega$ (10)

— due to the spin-photon coupling, the frequencies of the normal modes repulse from each other, while the normal decay rate is the same for the both modes, giving the complex frequency

$$\omega_{\pm}(LAC)=\omega_0 \pm \sqrt{\left(\Omega_R^{i-j}\right)^2-\left(\frac{\tau_c^{-1}-T_2^{-1}}{2}\right)^2}+i\frac{\tau_c^{-1}+T_2^{-1}}{2}, \tag{11}$$

which coincides with the results of Refs. of Thompson et al., (1992), Zhu et al., (1990), Diniz et al., (2011).

If $4\Omega_R^2<\left(\tau_c^{-1}-T_2^{-1}\right)^2$, then

$\Delta_{LAC}^{'}=0$ ($\omega_{\pm}^{'}=\omega_{LAC}=\omega_0$): $\Delta_{LAC}^{''}=\left[(\theta_1+\theta_2)\pm\sqrt{(\theta_1-\theta_2)^2-4\alpha_1\alpha_2}\right]/2$ or explicitly

$$\omega_{\pm}^{''}(LAC)=\frac{\tau_c^{-1}+T_2^{-1}}{2}\pm\sqrt{\left(\frac{\tau_c^{-1}-T_2^{-1}}{2}\right)^2-\Omega_R^2} \tag{12}$$

— the emitter and cavity frequencies stay unchanged, while the normal decay rates merge as a result of the spin-photon coupling, see Figure 2:

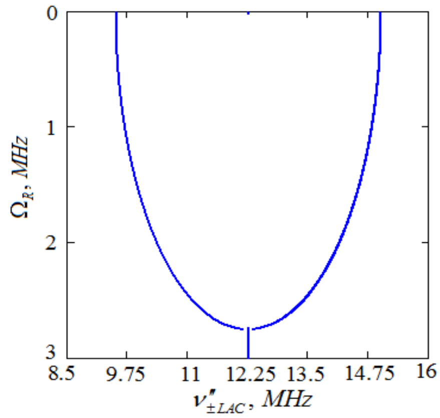

Figure 2. Predicted dependence of the normal decay rates $\nu_{\pm}^{''}(LAC)$ on Ω_R plotted according to Eq. (12) of the given paper. For the emitter and cavity decay rates the optional values $T_2^{-1}=2\pi\times 9.5MHz$; $\tau_c^{-1}=2\pi\times 15MHz$ are taken

SPIN-CAVITY POLARITON STUDY BY MEANS OF EPR SIGNALS AND CAVITY TRANSMISSION FUNCTION

Since EPR is one of the experimental methods of polariton investigation (see, for instance, Ref. of Salikhov et al (2023), where EPR of spin polaritons in a dilute solution of paramagnetic particles was observed), it is of interest to analytically obtain absorption and dispersion signals of spin-cavity polaritons to a weak (non-saturating) probe field. For this purpose, the classical approach in the linear approximation is valid (Thompson et al., 1992; Zhu et al., 1990). The solution of (3) in terms of Migulin et al. (1978) was sought in the form

$$h_{\mathbf{K}}^{i-j}=h_{\mathbf{K}}^{i-j}(probe)/\left(R_{eqv}+iX_{eqv}\right) \text{ with } R_{eqv}^{-1}=\frac{\theta_0^2+\Delta_{p0}^2}{\theta_c\left(\theta_0^2+\Delta_{p0}^2\right)+\alpha_1\alpha_2\theta_0}; \quad X_{eqv}=\Delta_{pc}-\frac{\alpha_1\alpha_2\Delta_{p0}}{\theta_0^2+\Delta_{p0}^2}, \tag{13}$$

where the resonance condition is $X_{eqv}=0$ (Migulin et al., 1978), which is satisfied by the three values of detuning:

$$\Delta_{p0}(I)=0;\ \Delta_{p0}(II,III)=\pm\sqrt{\alpha_1\alpha_2-\theta_0^2}\ . \tag{14}$$

The solutions $\Delta_{p0}\left(II,III\right)=\pm\sqrt{\alpha_1\alpha_2-\theta_{p0}^2}$ are valid, if $\alpha_1\alpha_2>\theta_{p0}^2$, these solutions correspond to the case of the unbroken symmetry regime in terms of Ref. (Dengke Zhang et al., 2017); the solution $\Delta_{p0}\left(I\right)=0$ is valid at $\alpha_1\alpha_2<\theta_{p0}^2$ and corresponds to the broken symmetry regime in the same terms. Transition from unbroken symmetry to broken symmetry and vice versa occurs at the coupling value $\alpha_1\alpha_2=\theta_{p0}^2$ (critical point in terms of Migulin et al., 1978), which corresponds to the exceptional point studied in detail in Ref. (Dengke Zhang et al., 2017). In the Figure 3, the consequences of solutions of Eq. (14) are presented in the form of $\nu_p(I,II,III)-\nu_0$ dependence on Ω_R.

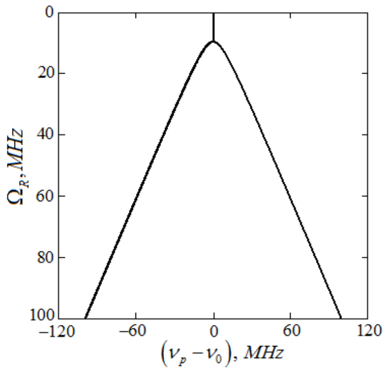

Figure 3. Dependence on Ω_R of the detuning $\nu_p(I,II,III)-\nu_0$ of the resonance probe field ($\nu_p=\nu_p(I,II,III)$) from the emitter frequency ν_0, according to (14). For the emitter decay rate the optional value $T_2^{-1}=2\pi\times 9.5MHz$ is taken.

It should be noted that the Fig. 3a from Ref. (Dengke Zhang et al., 2017), where the absolute value of the displacement x is the measure of the magnon-cavity coupling strength g_m, is essentially our Figure 3 rotated by π/2 and provided by its mirror reflection due to the specifics of their experiment. In the Fig. 3a from Ref. (Dengke Zhang et al., 2017), the exceptional points have coordinates ($x=\pm 1.2mm,\quad g_m/2\pi\approx 1.3|x|=\gamma_m/2\pi\approx 1.5MHz$); in our Figure 3, the critical point corresponds to the value $\Omega_R=T_2^{-1}$, where all three possible resonances coincide with each other, — the accordance with (Dengke Zhang et al., 2017) is clearly seen.

In the linear approximation we have obtained the following general formulae for the dispersion and absorption EPR signals for the case, when at an empty cavity is exactly tuned to the *i-j* transition of emitters ($\omega_c=\omega_0$, hereafter only this case is considered):

$$\chi^{'}=\frac{\alpha_1\alpha_2\left(\theta_0R_{eqv}-\Delta_{p0}X_{eqv}\right)}{\eta_0\left(\theta_0^2+\Delta_{p0}^2\right)\left(R_{eqv}^2+X_{eqv}^2\right)};\qquad \chi^{"}=\frac{\alpha_1\alpha_2\left(\Delta_{p0}R_{eqv}+\theta_0X_{eqv}\right)}{\eta_0\left(\theta_0^2+\Delta_{p0}^2\right)\left(R_{eqv}^2+X_{eqv}^2\right)},\tag{15}$$

where R_{eqv},X_{eqv} are defined by Eq. (13). Resonance condition of EPR signals reads as: $X_{eqv}=0$ (Migulin et al, 1978), giving the three possible values (I,II,III) of the resonance frequency of the probe field

$$\omega_p\left(I\right)=\omega_0;\quad \omega_p^2\left(II,III\right)=\frac{\omega_0^2}{1m\ \sqrt{\alpha_1\alpha_2-\theta_0^2}}.\tag{16}$$

1) In the case $\alpha_1\alpha_2 < \theta_0^2$ there is only one resonance frequency I. The corresponding steady-state EPR signals nearby this I resonance appeared to have the form:

$$\chi^{"}\left(\Delta_{p0} \approx 0, noncritical\right) \approx \frac{\alpha_1\alpha_2\Delta_{p0}\left(\theta_c + \theta_0\right)}{\eta_0\left(\theta_0^2 + \Delta_{p0}^2\right)\left(\theta_c^2 + \Delta_{p0}^2\right)}; \chi^{'}\left(\Delta_{p0} \approx 0, noncritical\right) \approx \frac{\alpha_1\alpha_2\left(\theta_c\theta_0\right)}{\eta_0\left(\theta_0^2 + \Delta_{p0}^2\right)\left(\theta_c^2 + \Delta_{p0}^2\right)} \quad (17)$$

where absorption signal has the dispersion form, while dispersion signal has the absorption form.

2) In the case $\alpha_1\alpha_2 \geq \theta_0^2$ two side peaks II, III (see Figure 4) appear in the EPR spectrum in addition to I resonance, the latter now being a minimum of EPR signals at halfway between side peaks (Migulin et al, 1978). At $\alpha_1\alpha_2 >> \theta_0^2, \theta_c\theta_0$ these peaks have the Lorentzian form with the FWHM$\left(\theta_c + \theta_0\right)$:

$$\chi^{"}\left(\Delta_{p0} \approx m\sqrt{\alpha_1\alpha_2}\right) \approx m\frac{\sqrt{\alpha_1\alpha_2}\left(\theta_c + \theta_0\right)/4}{\eta_0\left[\left(\theta_c + \theta_0\right)^2/4 + \left(\Delta_{p0} \pm \sqrt{\alpha_1\alpha_2}\right)^2\right]}; \quad (18)$$

$$\chi^{'}\left(\Delta_{p0} \approx m\sqrt{\alpha_1\alpha_2}\right) \approx \frac{\theta_0\left(\theta_c + \theta_0\right)/4}{\eta_0\left[\left(\theta_c + \theta_0\right)^2/4 + \left(\Delta_{p0} \pm \sqrt{\alpha_1\alpha_2}\right)^2\right]}. \quad (19)$$

3) The point $\alpha_1\alpha_2 = \theta_0^2$ is critical — there all three resonances coincide with each other and have the features of 1) resonance:

$$\chi^{'}\left(\Delta_{p0} \approx 0, critical\right) \approx \frac{\theta_0^3}{\eta_0\left(\theta_0^2 + \Delta_{p0}^2\right)\left(\theta_c + \theta_0\right)}; \quad \chi^{"}\left(\Delta_{p0} \approx 0, critical\right) \approx \frac{\Delta_{p0}\theta_0^2}{\eta_0\left(\theta_0^2 + \Delta_{p0}^2\right)\left(\theta_c + \theta_0\right)} \quad (20)$$

It is interesting to note that though Eqs. (17) and (20) describe EPR signals at the same detunings of the probe field, the predicted values of signals are different, since signals (17) correspond to the low-coupling end of the forks handle of Figure 3, while signals (20) correspond to the stronger-coupling end of the forks handle.

The general formulae of EPR absorption and dispersion signals, obtained by us for the case 2), have the following form:

$$\chi^{"}(peaks) \approx \frac{1}{\eta_0}\left\{\frac{\Omega_R^4\sqrt{\Omega_R^2 - \left(T_2^{-1}\right)^2}\left(T_2^{-1} + \tau_c^{-1}\right)}{\Omega_R^4\left(T_2^{-1} + \tau_c^{-1}\right)^2 + 4\left[\Omega_R^2 - \left(T_2^{-1}\right)^2\right]^2\left(\omega_p - \omega_0 - \sqrt{\Omega_R^2 - \left(T_2^{-1}\right)^2}\right)^2} - \right.$$

$$\left. - \frac{\Omega_R^4\sqrt{\Omega_R^2 - \left(T_2^{-1}\right)^2}\left(T_2^{-1} + \tau_c^{-1}\right)}{\Omega_R^4\left(T_2^{-1} + \tau_c^{-1}\right)^2 + 4\left[\Omega_R^2 - \left(T_2^{-1}\right)^2\right]^2\left(\omega_p - \omega_0 + \sqrt{\Omega_R^2 - \left(T_2^{-1}\right)^2}\right)^2}\right\};$$

(21)

$$\chi' = \frac{1}{\eta_0}\left\{ \frac{\Omega_R^4\left(-2\left[\omega_p-\omega_0-\sqrt{\Omega_R^2-T_2^{-2}}\right]\sqrt{\Omega_R^2-T_2^{-2}}+T_2^{-1}\left(T_2^{-1}+\tau_c^{-1}\right)\right)}{\Omega_R^4\left(T_2^{-1}+\tau_c^{-1}\right)^2+4\left(\Omega_R^2-T_2^{-2}\right)^2\left[\omega_p-\omega_0-\sqrt{\Omega_R^2-T_2^{-2}}\right]^2} + \right.$$
$$\left. + \frac{\Omega_R^4\left(2\left[\omega_p-\omega_0+\sqrt{\Omega_R^2-T_2^{-2}}\right]\sqrt{\Omega_R^2-T_2^{-2}}+T_2^{-1}\left(T_2^{-1}+\tau_c^{-1}\right)\right)}{\Omega_R^4\left(T_2^{-1}+\tau_c^{-1}\right)^2+4\left(\Omega_R^2-T_2^{-2}\right)^2\left[\omega_p-\omega_0+\sqrt{\Omega_R^2-T_2^{-2}}\right]^2} \right\}. \tag{22}$$

The plots, constructed according to the Eqs. (21) and (22) of the given paper and scaled in the units of the instrumental factor η_0, are shown in the following Figure 4:

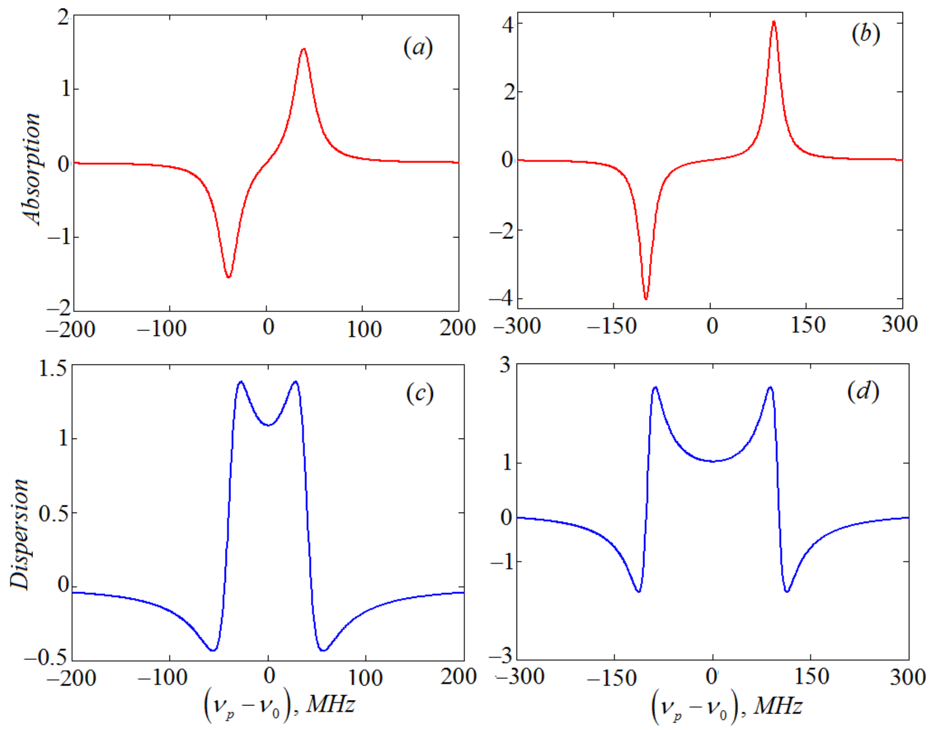

Figure 4. EPR signals plotted according to the Eqs. (21) and (22) of the given paper and scaled in the units of the instrumental factor η_0: (a), (b) – absorption signals; (c), (d) dispersion signals, both for the optional values of the parameters: decay rates $\tau_c^{-1} = 2\pi\times 15MHz$ (for cavity) and $T_2^{-1} = 2\pi\times 9.5MHz$ (for emitters); Rabi frequency for (a) and (c) is $\Omega_R = 2\pi\times 40MHz$; for (b) and (d) is $\Omega_R = 2\pi\times 100MHz$

However, the observation of the transmission function (TF) of a cavity with *N* emitters in it is seemingly the best method to investigate polaritonic peaks (Thompson et al., 1992; Zhu et al., 1990). TF $T(\omega_p) = |t(\omega_p)|^2$ for a weak probe field is the ratio of the energy, transmitted through the cavity, to that of the incident on it. It appeared that the quantum-mechanical method of $t(\omega_p)$ calculation is more suitable now. So, using expressions (5, 6) from the Ref. of Diniz et al. (2011), the following general expression for $t(\omega_p)$ can be written:

$$t(\omega_p) = \frac{\tau_c^{-1}}{i}\frac{\omega_p-\omega_0+iT_2^{-1}}{\left(\omega_p-\omega_0+iT_2^{-1}\right)\left(\omega_p-\omega_c+i\tau_c^{-1}\right)-\Omega_R^2} \tag{23}$$

From (23), TF behavior in the particular areas of the parameters can be described:

At $\Omega_R^2 < T_2^{-1}\tau_c^{-1}, T_2^{-2}$,

$$\left|t(\omega)\right|^2 = \left[\frac{\tau_c^{-1}T_2^{-1}\left(\Omega_R^2 + T_2^{-1}\tau_c^{-1}\right)}{\left[(\omega-\omega_0)^2 - \Omega_R^2 - T_2^{-1}\tau_c^{-1}\right]^2 + (\omega-\omega_0)^2\left(T_2^{-1}+\tau_c^{-1}\right)^2}\right]^2, \quad (24)$$

i.e. TF is a Lorentzian squared having poles at $\omega_0 - i\left[\frac{T_2^{-1}+\tau_c^{-1}}{2} \pm \sqrt{\left(\frac{T_2^{-1}+\tau_c^{-1}}{2}\right)^2 - \Omega_R^2 - T_2^{-1}\tau_c^{-1}}\right]$, while

at $\Omega_R^2 > T_2^{-1}\tau_c^{-1}, T_2^{-2}$

$$\left|t(\omega\approx\omega_+)\right|^2 + \left|t(\omega\approx\omega_-)\right|^2 = \frac{\Omega_R^2 + T_2^{-1}\tau_c^{-1} + T_2^{-2}}{4\left(\Omega_R^2 + T_2^{-1}\tau_c^{-1}\right)} \times$$

$$\times\left\{\left[\frac{\tau_c^{-1}\left(T_2^{-1}+\tau_c^{-1}\right)/2}{\left[(\omega-\omega_0) - \sqrt{\Omega_R^2 + T_2^{-1}\tau_c^{-1}}\right]^2 + \left[\left(T_2^{-1}+\tau_c^{-1}\right)/2\right]^2}\right]^2 + \left[\frac{\tau_c^{-1}\left(T_2^{-1}+\tau_c^{-1}\right)/2}{\left[(\omega-\omega_0) + \sqrt{\Omega_R^2 + T_2^{-1}\tau_c^{-1}}\right]^2 + \left[\left(T_2^{-1}+\tau_c^{-1}\right)/2\right]^2}\right]^2\right\}$$

(25)

– each peak has the form of a squared Lorentzian with the decay $\left(T_2^{-1}+\tau_c^{-1}\right)/2$, at that, the resonance frequencies of these Lorentzians are $\omega_0 \pm \sqrt{\Omega_R^2 + T_2^{-1}\tau_c^{-1}}$. These features of TF, which are in accord with the Ref. of Zhu et al. (1990), are illustrated by Figure 5.

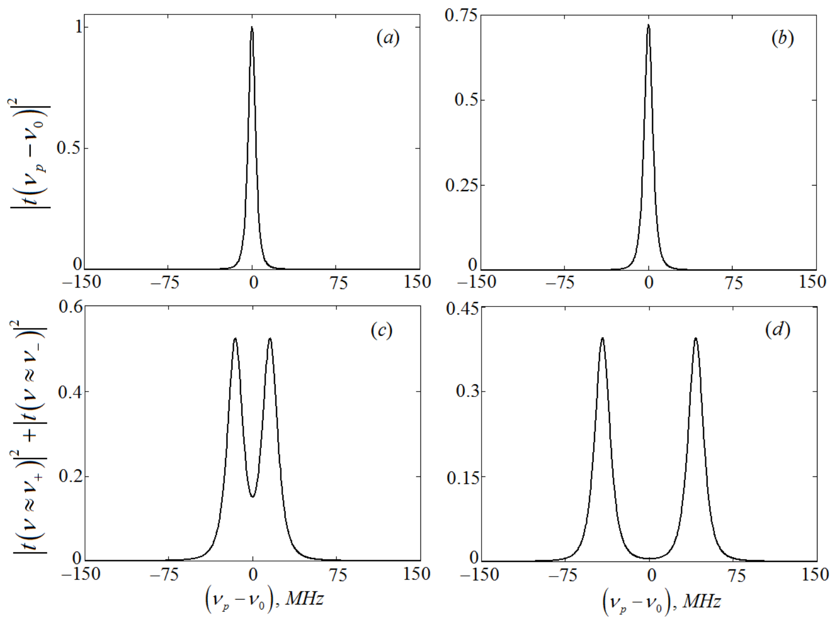

Figure 5. Intensity transmission function of the coupled atom-cavity system, plotted according to Eqs. (24) and (25) of the given paper. For the cavity decay rate the value $\tau_c^{-1} = 2\pi\times15MHz$ is taken, and for the EPR linewidth the value $T_2^{-1} = 2\pi\times9.5MHz$ is taken of $Ba\,6S^2\,{}^1S_0 - 6S6p\,{}^1P_1$ transition of an ensemble of barium atoms from Ref. of Zhu et al. (1990). Plots are constructed for different Rabi frequencies: (a) $\Omega_R = 0MHz$; (b) $\Omega_R = 2\pi\times5MHz$; (c) $\Omega_R = 2\pi\times10MHz$; (d) $\Omega_R = 2\pi\times40MHz$

RESULTS AND DISCUSSION

The significance of the results of this paper lies in the fact that in it the values directly measured in various types of experiments are presented in a simple and clear form via experimental parameters for any emitter-cavity polaritons. At that, a variety of two-level systems (spin transitions, magnons, atoms, molecules, excitons and so on) can act as emitters. The “fork” effect is predicted for normal decays at the decreasing of the value of the spin-photon coupling, in contrast to the known “fork” effect of normal frequencies with increasing spin-photon coupling. The latter effect qualitatively repeats the results of the skilful experiments of Ref. (Dengke Zhang et al., 2017), which were interpreted there quantum-mechanically, as a result of a phase transition between the states with the different symmetry of the quantum Hamiltonians. Our research shows that the classical approach in the linear approximation is well suited for solving the stated problems. However, it should be mentioned that the so-called “cavity protection” effect, associated with non-Markovian memory effects and inhomogeneous broadening of spin transition with non-Lorentzian lineshapes, could not be described in our linear approximation ─ this is the expected limitation of our method.

CONCLUSION

In the given paper, it was demonstrated that a lot of features of polariton peaks from the coupled system "emitters + cavity" can be successfully considered classically in the linear approximation: pushing aside of the normal frequencies of free oscillations of this coupled system at the increase of the coupling strength; merging together of the normal decays of free oscillations of this coupled system at such increase (to the best of our knowledge, first predicted here by us); manifestations of polaritonic peaks in EPR in the form of opposite in sign absorption signals divided by the double Rabi frequency; manifestations of polaritonic peaks in intensity transmission function in the form of equal in sign signals, divided by the double Rabi frequency. What seems most surprising ─ the qualitative agreement with the ingenious experiments of Ref.(Dengke Zhang et al., 2017), which were interpreted there quantum-mechanically, as a result of a phase transition between the states with the different symmetry of the quantum Hamiltonians. Using the analytics of this article can help experimentalists successfully study emitter-cavity polaritons.

REFERENCES

Abragam A 2006. Principles of Nuclear Magnetism. Oxford: Oxford University Press, 599pp.

Breeze J, Salvadori E, Sathian J, Alford N, Kay Ch 2017. Room-temperature cavity quantum electrodynamics with strongly coupled Dicke states. npj Quantum Information, 3:40.

Diniz I, Portolan S, Ferreira R, Gerard JM, Bertet P, Auffeves A 2011. Strongly coupling a cavity to inhomogeneous ensembles of emitters: potential for long lived solid-state quantum memories. Phys. Rev. A, 84: 063810.

Fokina N and Elizbarashvili M 2022. Pure Superradiance at the Inhomogeneous Broadening of Inverted Transitions of Spin-Triplet States. International Conference on Global Practice of Multidisciplinary Scientific Studies, Proceeding book, 437-447.

Fokina N and Elizbarashvili M 2021. Pure Superradiance from the Inverted Levels of Spin Triplet States Coupled to Resonator. Appl. Mag. Reson., 52:769-780.

Haroche S and Raimond JM 2006. Exploring the Quantum Atoms, Cavities and Photons. Oxford: Oxford University Press, 605 pp.

Migulin VV, Medvedev VI, Mustel ER, Parygin VN 1978. Basic Theory of Oscillations (in Russian). Moscow: Nauka, 392 pp.

Salikhov KM, Bakirov MM, Zaripov RB, Khairutdinov IT 2023. Experimental confirmation of the formation of a spin polariton in dilute solutions of paramagnetic particles. Phys. Chem. Chem. Phys., 25: 17966–17977.

Thompson R J, Rempe G, Kimble HJ 1992. Observation of normal-mode splitting for an atom in an optical cavity. Phys. Rev. Lett. 68: 1132-1135.

Zhang Dengke, Luo X-Q, Wang Y-P, Li T-F, You JQ 2017. Observation of the exceptional point in cavity magnon-polaritons. Nature Communications. 8:1368

Zhu Y, Gauthier DJ, Morin SE., Wu Q, Carmichael H J, Mossberg TW 1990.Vacuum Rabi splitting as a feature of linear-dispersion theory: Analysis and experimental observations. Phys. Rev. Lett. 64: 2499-2502.